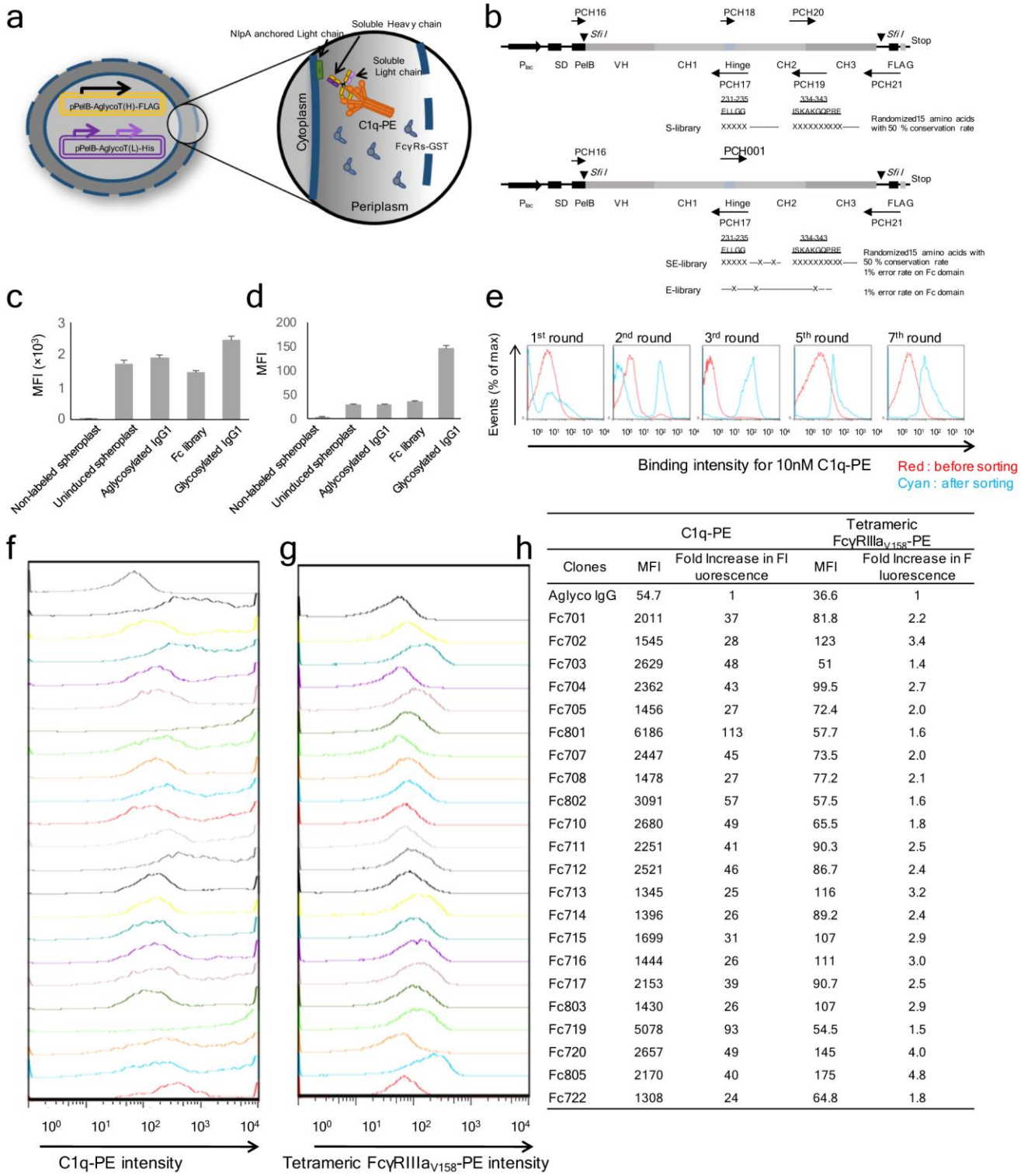

Clones	C1q-PE MFI	C1q-PE Fold Increase in Fluorescence	Tetrameric FcγRIIIa$_{V158}$-PE MFI	Tetrameric FcγRIIIa$_{V158}$-PE Fold Increase in Fluorescence
Aglyco IgG	54.7	1	36.6	1
Fc701	2011	37	81.8	2.2
Fc702	1545	28	123	3.4
Fc703	2629	48	51	1.4
Fc704	2362	43	99.5	2.7
Fc705	1456	27	72.4	2.0
Fc801	6186	113	57.7	1.6
Fc707	2447	45	73.5	2.0
Fc708	1478	27	77.2	2.1
Fc802	3091	57	57.5	1.6
Fc710	2680	49	65.5	1.8
Fc711	2251	41	90.3	2.5
Fc712	2521	46	86.7	2.4
Fc713	1345	25	116	3.2
Fc714	1396	26	89.2	2.4
Fc715	1699	31	107	2.9
Fc716	1444	26	111	3.0
Fc717	2153	39	90.7	2.5
Fc803	1430	26	107	2.9
Fc719	5078	93	54.5	1.5
Fc720	2657	49	145	4.0
Fc805	2170	40	175	4.8
Fc722	1308	24	64.8	1.8

Supplementary Figure 1

Engineering of C1q-specific IgG antibodies.

(**a**) Schematic illustration of aglycosylated IgG display system for Fc engineering. Soluble C1q-PE competes with non-fluorescent FcγRs-GST for

binding to the displayed IgG variants on the surface of bacterial spheroplasts before FACS sorting. (**b**) Schematic illustration of the construction of the three sub-libraries of mutated Fc domains: S-library: randomization of the focused 15 amino acids; E-library: random mutagenesis on Fc domain by error prone PCR with 1% error rate: SE-library: random mutagenesis of the S-library gene pool by error prone PCR with 1% error rate. The sizes of sub-libraries were 2×10^8 (S-library), 3×10^8 (SE-library), and 1×10^9 (E-library). (**c**) C1q does not bind to IgG-displaying *E.coli* spheroplasts in high salt buffer (50 mM phosphate, 330 mM NaCl, pH 7.4). Since *E.coli* cannot synthesize glycosylated antibodies, *E.coli* cells were engineered to display an antigen (PA domain 4) on the inner membrane and then the spheroplasted cells were incubated with the very high affinity anti-PA domain 4 antibody, M18. Binding to C1q to the surface-bound C1q was detected by FACS using 10 nM C1q-PE. (**d**) Flow cytometry analysis of C1q binding onto IgG-displaying *E.coli* spheroplasts in high salt buffer. (**e**) Flow cytometry analysis of *E.coli* library spheroplasts labeled with 10 nM C1q-PE before (Red) and after sorting (Cyan). (**f-g**) Fluorescent histogram of isolated IgG variants binding to 10 nM of C1q-PE in high salt phosphate buffer (**f**) or to 10 nM of tetrameric FcγRIIIa$_{V158}$-PE in PBS (**g**). (**h**) MFI and fold increase in MFI following incubation with C1q or tetrameric FcγRIIIa$_{V158}$ relative to cells unmutated aglycosylated IgG.

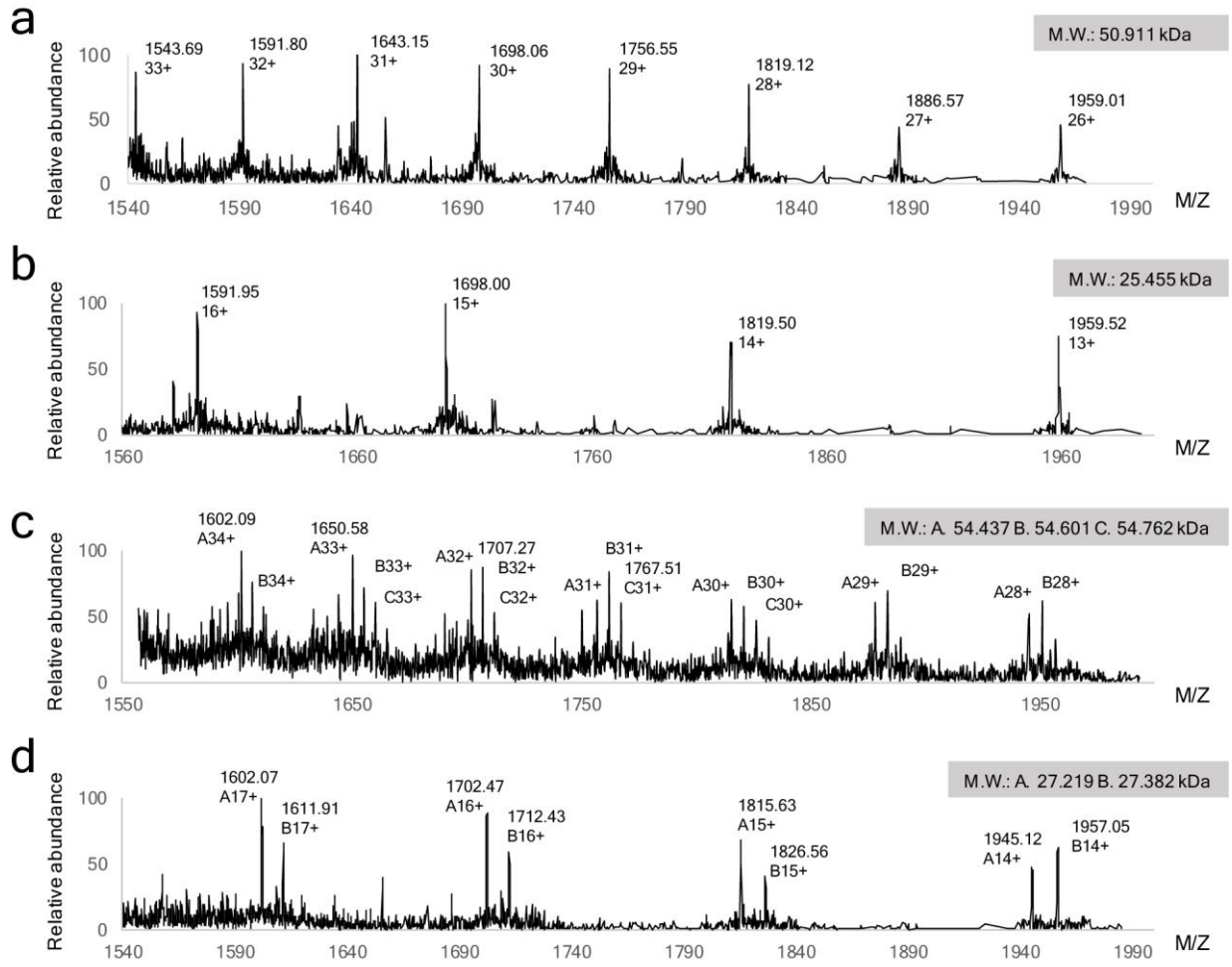

Supplementary Figure 2

LC-MS/MS spectra of 801 Fc.

Purified A801 Fc (**a-b**) or G801 Fc (**c-d**) was examined without (**a** & **c**) or with (**b** & **d**) 160 mM of dithiothreitol (DTT). Molecular weight (M.W.) estimated from the LS-MS data are shown; the respective calculated masses were presented at top of each plot. In (**c**) and (**d**) multiple predominant species detected are a consequence of glycan heterogeneity.

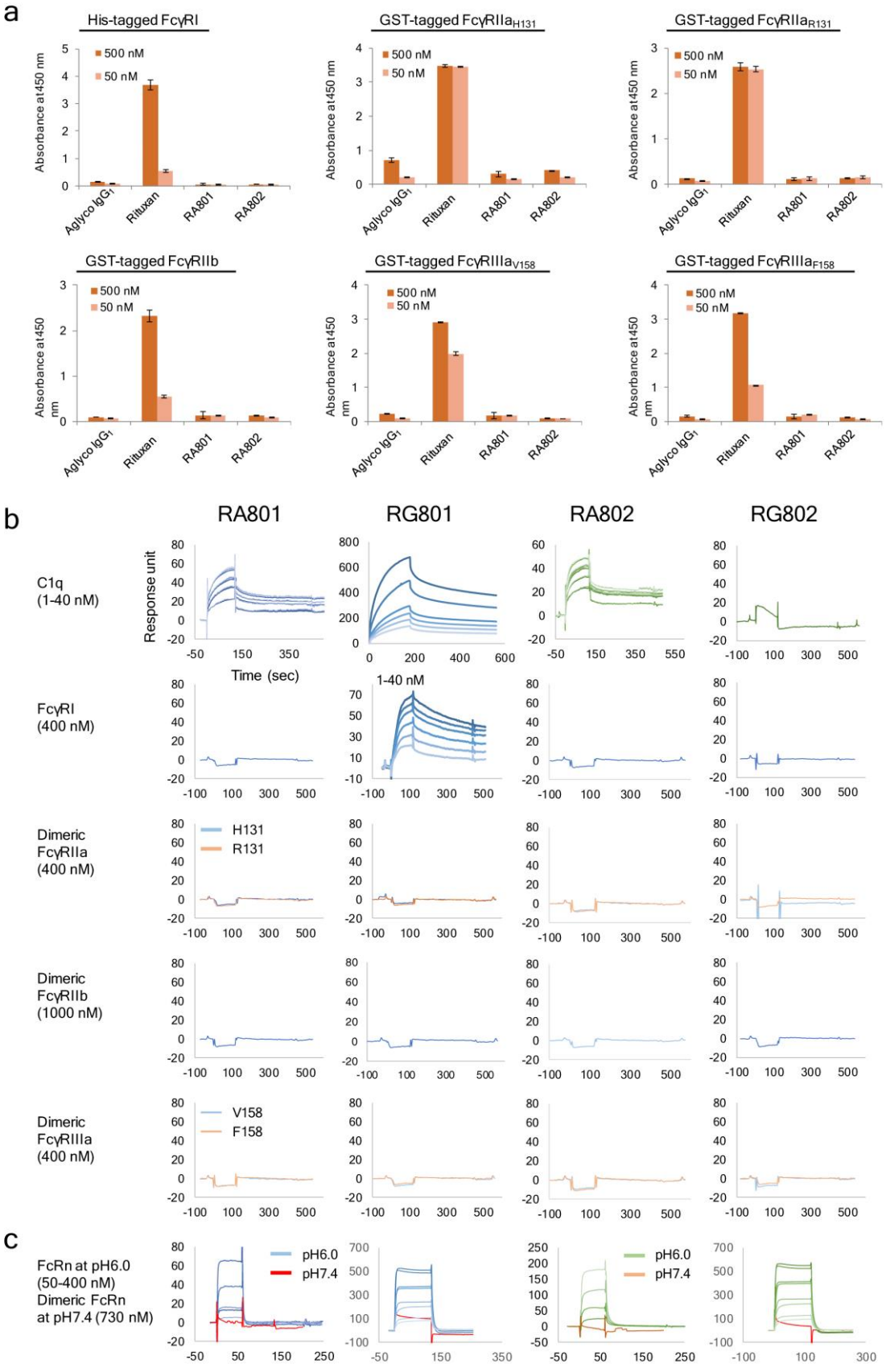
a
His-tagged FcγRI
GST-tagged FcγRIIa$_{H131}$
GST-tagged FcγRIIa$_{R131}$
GST-tagged FcγRIIb
GST-tagged FcγRIIIa$_{V158}$
GST-tagged FcγRIIIa$_{F158}$
Absorbance at450 nm
500 nM
50 nM
Aglyco IgG$_1$
Rituxan
RA801
RA802
b
RA801
RG801
RA802
RG802
C1q
(1-40 nM)
Response unit
Time (sec)
FcγRI
(400 nM)
1-40 nM
Dimeric
FcγRIIa
(400 nM)
H131
R131
Dimeric
FcγRIIb
(1000 nM)
Dimeric
FcγRIIIa
(400 nM)
V158
F158
c
FcRn at pH6.0
(50-400 nM)
Dimeric FcRn
at pH7.4 (730 nM)
pH6.0
pH7.4

Supplementary Figure 3

Binding analysis of RA801 or RA802 to human C1q, FcγRs and FcRn.

(**a**) ELISA analysis of C1q-specific antibody variants binding to human FcγRs. ELISA plates were coated with aglycosylated IgG1 (negative control), glycosylated IgG1 (Rituxan, positive control), RA801 or RA802. 500 nM or 50 nM of his-tagged FcγRI, GST-tagged $FcγRIIa_{H131}$, GST-tagged $FcγRIIa_{R131}$, GST-tagged FcγRIIb, GST-tagged $FcγRIIIa_{V158}$, or GST-tagged $FcγRIIIa_{F158}$ was added and binding was detected using anti-His IgG conjugated to HRP or anti-GST IgG-HRP, accordingly. Errors bars: standard deviations from triplicate experiments. (**b**-**c**) SPR analysis of C1q-specific antibody variants. (**b**) SPR analysis of antibody binding to purified C1q or to effector Fcγ receptors. Antibody variants were immobilized on CM5 chips. The binding of C1q, or of GST fusion proteins high affinity FcγRI, or low affinity FcγRIIa, FcγRIIb, or FcγRIIIa, all expressed as dimers, to enhance binding, was assayed. (**c**) pH-dependent binding to human FcRn. In all sensorgrams, x-axis is time (sec) and y-axis is RU (response unit). Data are from one experiment representative of three experiments (**a**-**c**).

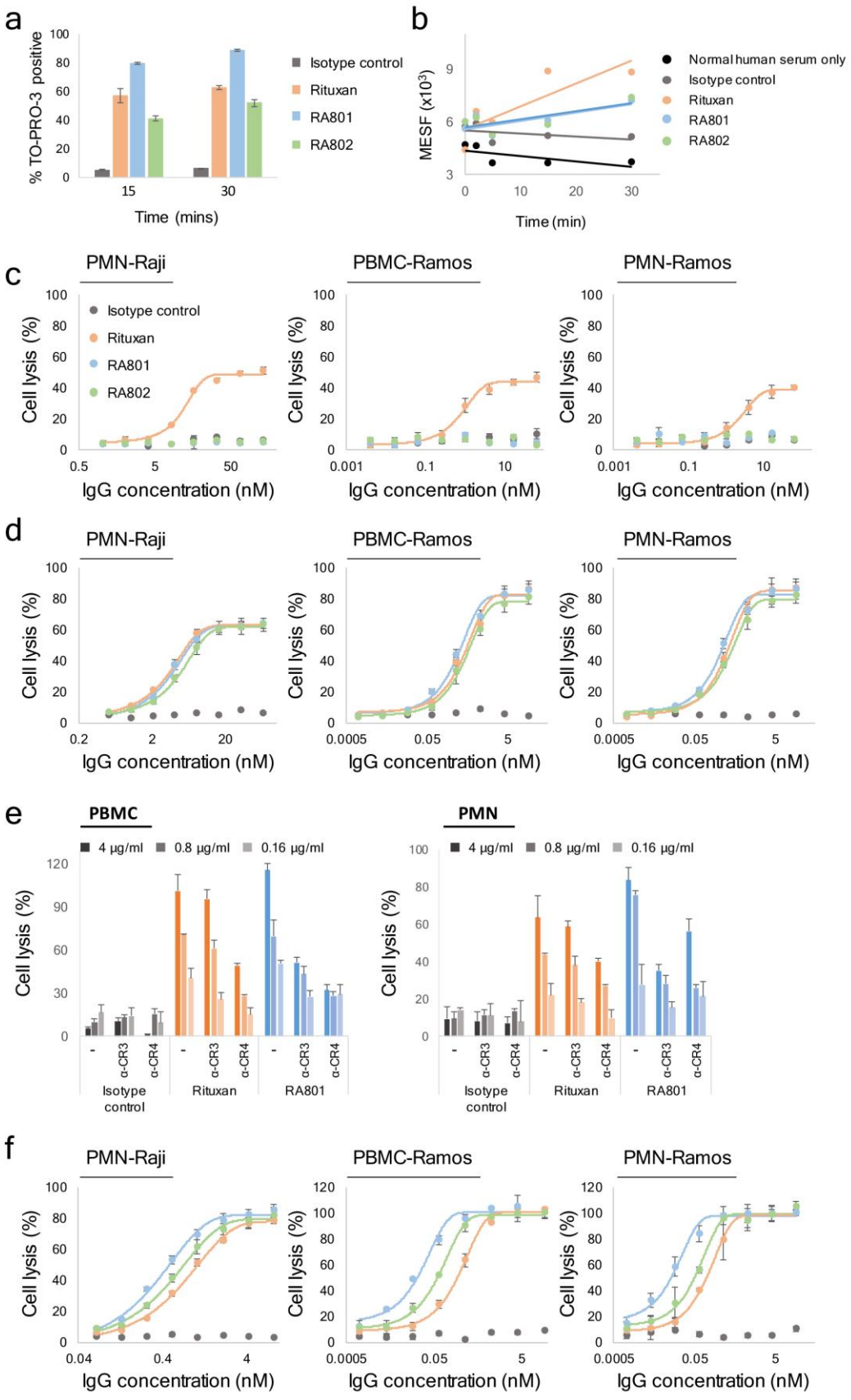
a
% TO-PRO-3 positive
Time (mins)
Isotype control
Rituxan
RA801
RA802
b
MESF (x10³)
Time (min)
Normal human serum only
Isotype control
Rituxan
RA801
RA802
c
PMN-Raji
PBMC-Ramos
PMN-Ramos
Cell lysis (%)
IgG concentration (nM)
d
e
PBMC
PMN
4 µg/ml
0.8 µg/ml
0.16 µg/ml
α-CR3
α-CR4
Isotype control
Rituxan
RA801
f

Supplementary Figure 4

Complement-mediated tumor-cell killing by C1q-specific antibody variants.

(**a**) CDC assays with Daudi cells. 10 μg/ml of each antibody was incubated with 50 % of PHS and $CD20^+$ Daudi cells for 15 mins and 30 mins. Lysed cells were detected by TO-PRO-3. (**b**) C1q deposition on mAb-opsonized $CD20^+$ cells. Time course for C1q deposition on $CD20^+$ Raji cells. Raji cells were incubated in 5% NHS and 10 μg/ml mAb for different time periods at 37°C. Cells were washed twice, incubated with FITC-conjugated anti-C1q and assayed by flow cytometry. MFI were converted to molecules of equivalent soluble fluorochrome (MESF) using calibrated beads (Spherotech). (**c-d**) $CD20^+$ cancer cells killing activities by PBMC or PMNs. Raji (or Ramos) cells incubated with effector cells in RPMI1640 medium without serum (**c**) or with 25% of C9-depleted serum (**d**). (**e**) Effect of α-CR3 or α-CR4 antibodies in CDCC. Rituximab (or RA801)-opsonized Ramos cells were incubated with: 10μg/ml of α-CR3 Ab (or α-CR4 Ab)-coated effector cells in RPMI1640 medium supplemented with 25% C9-depleted serum. (**f**) Cell killing of $CD20^+$ cancer cells by effector cells in the presence of serum. Cell lysis of $CD20^+$ cells with effector cells in RPMI1640 medium supplemented with 25% PHS. In **c-f**, % of cell lysis was determined 4 hours after the addition of cells and antibody. In all assays, the percent of tumor cell lysis was calculated according to the following formula: 100 × (E-S)/(M-S), where E is the fluorescence of the experimental well, S is the fluorescence in the absence of antibody (tumor cells incubated with medium and complement alone), and M is that of tumor cells with lysis buffer (Triton® X-100 at 2% v/v, SDS at 1% w/v, 100 mM NaCl, and 1 mM EDTA). In all assays, PMN cells were stimulated by incubation with 10 ng/mL GM-CSF and trastuzumab-IgG was used as a negative control. Errors bars indicate the standard deviation (s.d.) from triplicate experiments. Data are from one experiment representative of three experiments.

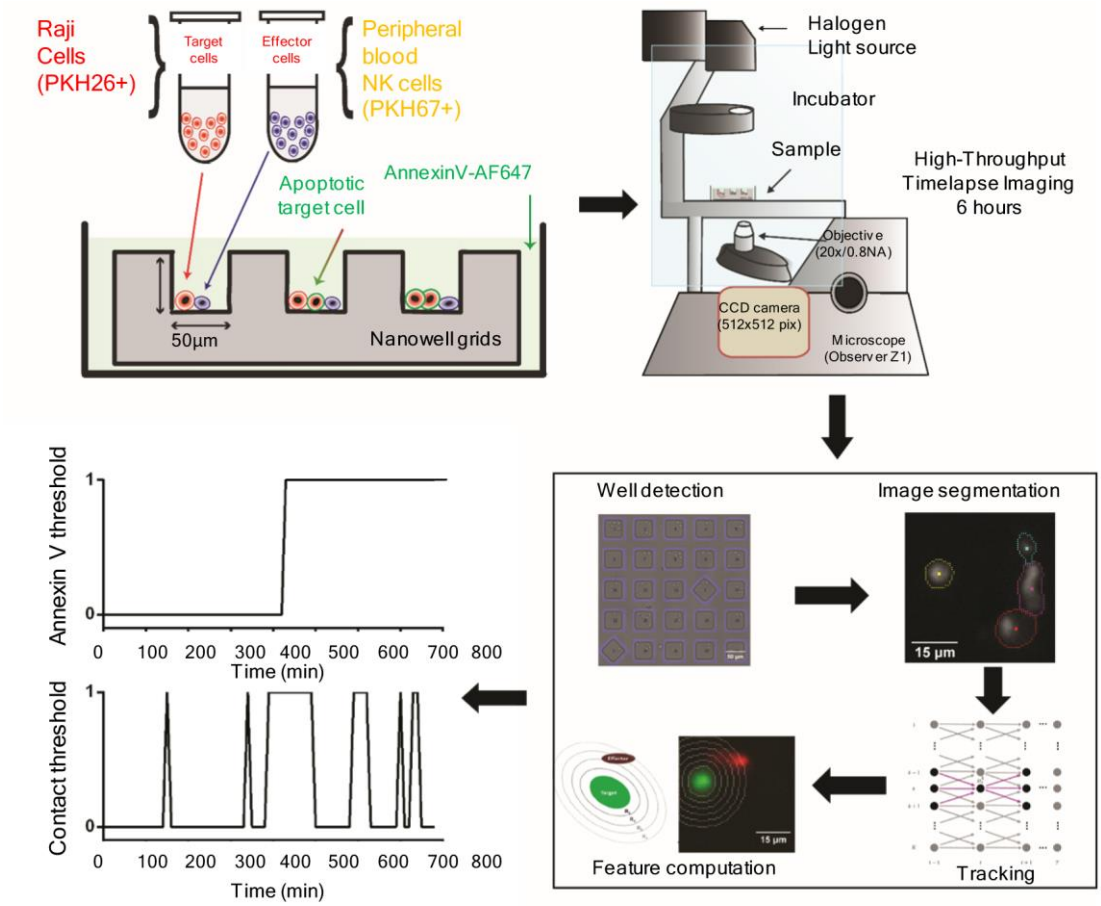

Supplementary Figure 5

Time-lapse imaging in nanowell grids (TIMING).

Raji tumor cells and NK cells are stained with PKH26 and PKH67 respectively, deposited *en masse* on a grid containing thousands of nanowells, immersed in fluorescent annexin V-containing medium and imaged for 6 h by high throughput timelapse microscopy. Imaging data were analyzed as described (Merouane Bioinformatics).

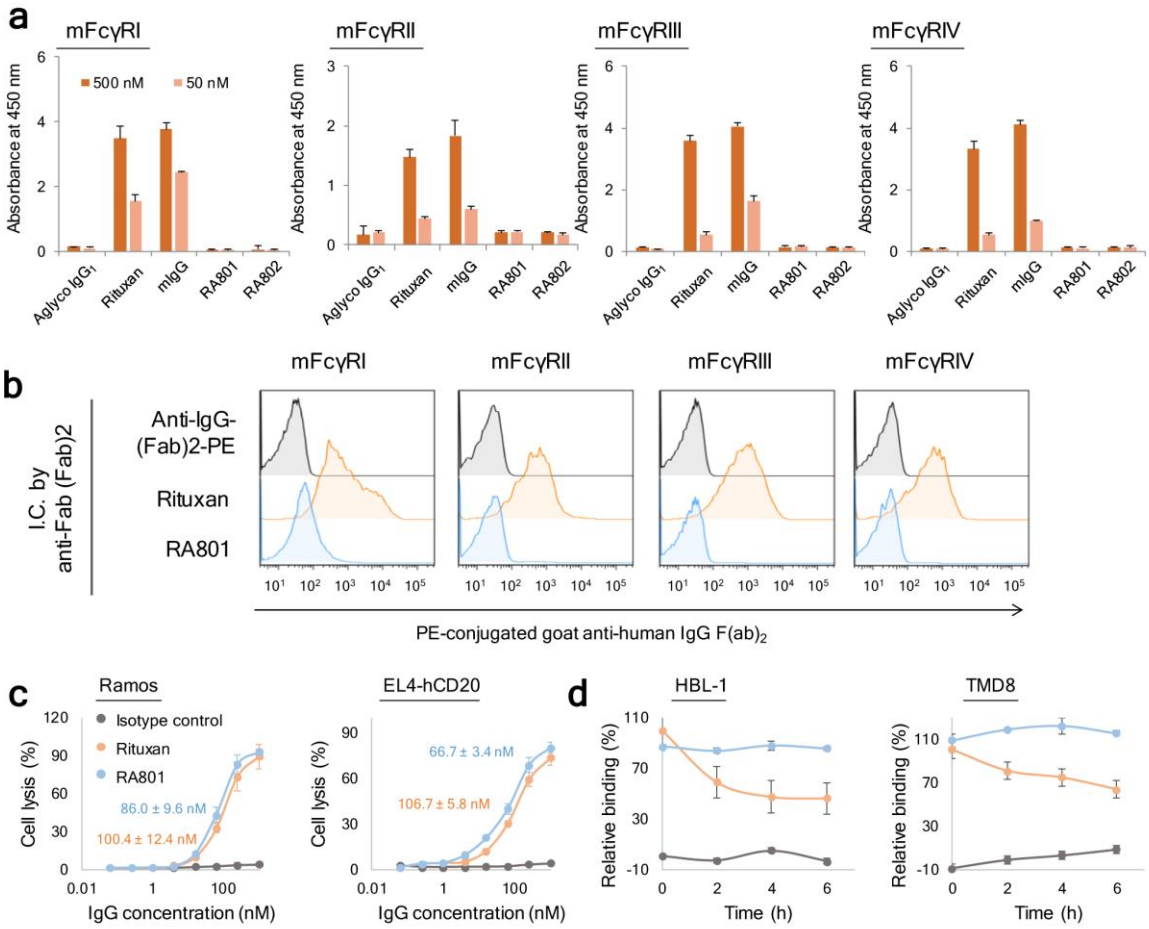

Supplementary Figure 6

Mouse complement activation of C1q-specific antibody variants and FcγR-mediated internalization in CD20$^+$FcγRIIb$^+$ cancer cells.

(**a**) Binding RA801 and RA802 to mouse FcγRs. Microtiter well plates were coated with aglycosylated IgG1 (negative control), glycosylated IgG1 (Rituxan, positive control), mIgG, RA801, or RA802. His-tagged mFcγRs were added and binding was detected using anti-His IgG conjugated to HRP. Errors bars: standard deviations from triplicate experiments. (**b**) Lack of binding of RA801 immune complexes to mouse FcγRs expressed on CHO cells. The binding activities of performed ICs made of RA801 or Rituxan with PE-conjugated F(ab')$_2$ goat anti-human IgG F(ab')$_2$. (**c**) CDC assays with pooled mouse serum (PMS)**.** CDC assays of CD20$^+$ cells by RA801 with PMS. Experimental conditions for CDC assays of Ramos cells as in **Supplementary Fig. 4.** Calcein-loaded EL4-hCD20 cells were incubated with 50 % of PMS and serially diluted antibodies for 4 hrs. EC_{50} values were presented in the plot (Orange: Rituxan, Blue: RA801). (**d**) α-CD20 antibody internalization in CD20$^+$FcγRIIb$^+$ cancer cells, HBL-1 or TMD8. CD20$^+$FcγRIIb$^+$ cancer cells were incubated with 100 nM of RA801 or RA802 for 0, 2, 4, or 6 h. Surface bound IgG was detected by flow cytometry using FITC conjugated goat anti-human Fc. (Abcam). In all assays, trastuzumab-IgG was used as a negative control and errors bars indicate the s.d. from triplicate experiments. Data are from one experiment representative of three experiments.

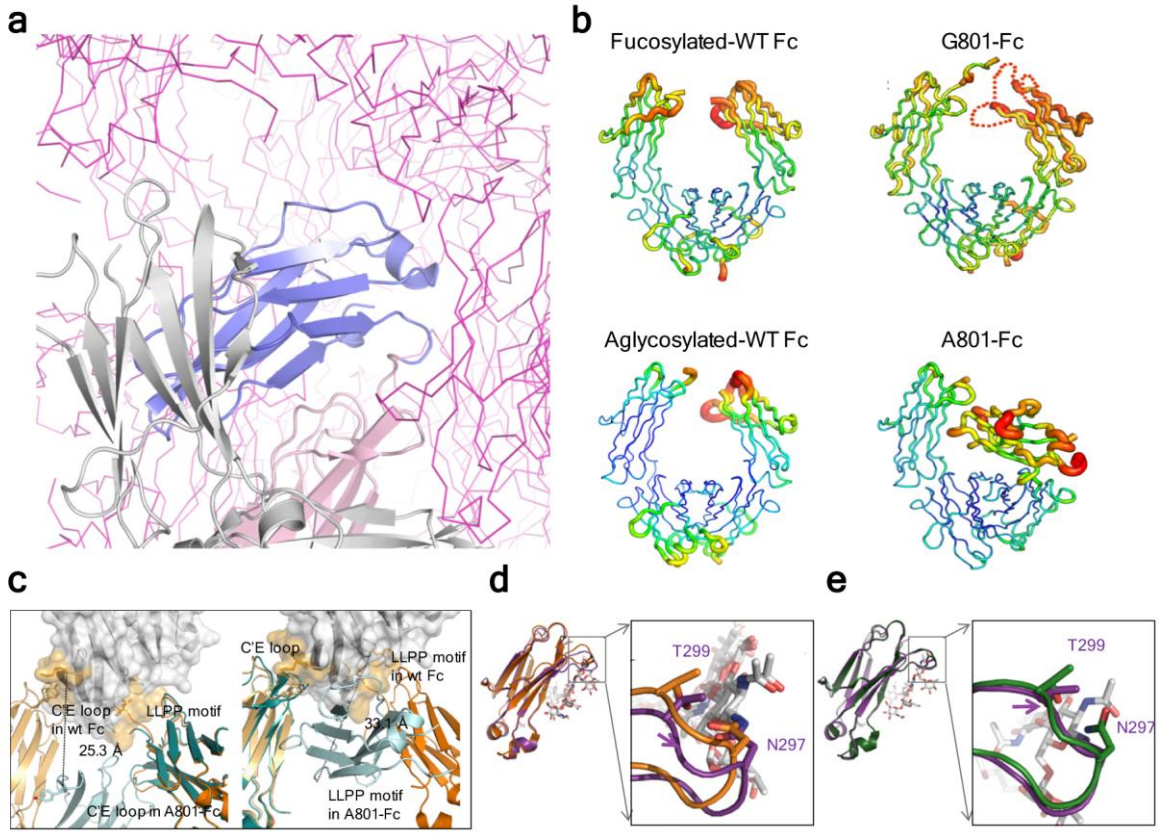

Supplementary Figure 7

Structural analysis of C1q-specific Fc variants.

(**a**) Crystal packing environment for A801-Fc. The crystallographic packing lattice is shown for A801-Fc (PDB ID: 5V43). The dimer from one asymmetric unit is shown in cartoon representation, with $C\gamma2_A$ in white; $C\gamma2_B$ in blue; and $C\gamma3_B$ in pink. Surrounding asymmetric units are shown in ribbon representation (magenta). No contacts or atomic clashes were observed between $C\gamma2_B$ and molecules from surrounding asymmetric units. (**b**) B factors distribution fucosylated-WT Fc (PDB ID: 3AVE), G801-Fc (PDB ID: 5V4E), aglycosylated-WT Fc (PDB ID: 3S7G), A801-Fc (PDB ID: 5V43). The coloring of the figure is based on the B factors gradient with lowest (blue) to highest (red). The dash line represents disordered regions. (**c**) Distance of FcγR-binding motifs of Fc domain to FcγRI (PDB ID: 4X4M). FcγR is shown as a white transparent surface and the secondary structure of the whole complex is shown in ribbon. Two different regions on the Fc are both identified to be important for FcγR and Fc complex formation: LLPP motif (important residue Leu235 is shown in sticks) and C'E loop. (**d-e**) Overlaid Cγ2 and 'soft' C'E loop of 801-Fc with wild type Fc. (**d**) Cγ2 of G801-Fc (PDB 5V4E, purple) was superimposed with fucosylated-WT Fc (orange, PDB: 3AVE). (**e**) G801-Fc (purple) was superimposed with aglycosylated-WT Fc (green, PDB: 3S7G). The 'soft' C'E loop of G801-Fc was highlighted by arrow. The glycan in PDB 3AVE is shown in white.

Supplementary Information

Supplementary Table 1. Primer list

Primer Name	Primer nucleotide sequence (5′→ 3′)
PCH001	CACCAAGGTCGACAAGAAAGTTG
PCH016	GTTATTACTCGCGGCCCAGCCG
PCH017	GGGGAAGAGGAAGACTGACGGN(A10% T70% G10% C10%)N(A10% T10% G10% C70%)N(A10% T10% G10% C70%)N(A10% T10% G10% C70%)N(A10% T10% G10% C70%)N(A10% T10% G10% C70%)N(A10% T10% G10% C70%)N(A70% T10% G10% C10%)N(A10% T10% G70% C10%)N(A10% T10% G70% C10%)N(A70% T10% G10% C10%)N(A10% T10% G70% C10%)N(A10% T70% G10% C10%)N(A10% T70% G10% C10%)N(A10% T10% G10% C70%)AGGTGCTGGGCACGGTGGG
PCH018	CCGTCAGTCTTCCTCTTCCCC
PCH019	GGTTTTCTCGATGGGGGCTGGG
PCH020	CCCAGCCCCCATCGAGAAAACCN(A70% T10% G10% C10%)N(A10% T70% G10% C10%)N(A10% T10% G10% C70%)N(A10% T70% G10% C10%)N(A10% T10% G10% C70%)N(A10% T10% G10% C70%)N(A70% T10% G10% C10%)N(A70% T10% G10% C10%)N(A70% T10% G10% C10%)N(A10% T10% G70% C10%)N(A10% T10% G10% C70%)N(A70% T10% G10% C10%)N(A70% T10% G10% C10%)N(A10% T10% G70% C10%)N(A10% T10% G70% C10%)N(A10% T10% G10% C70%)N(A70% T10% G10% C10%)N(A10% T10% G70% C10%)N(A10% T10% G10% C70%)N(A10% T10% G10% C70%)N(A10% T10% G10% C70%)N(A10% T10% G70% C10%)N(A70% T10% G10% C10%)N(A10% T10% G70% C10%)N(A70% T10% G10% C10%)N(A70% T10% G10% C10%)CCACAGGTGTACACCCTGCCC
PCH021	CGGCCGCGAATTCGGCCCC
PCH022	GGGGAAGAGGAAGACTGACGG
PCH023	GGTTTTCTCGATGGGGGCTGGG
mFcγRI F	CCC AAG CTT GAA GTG GTT AAT GCC ACC AAG GCT G

mFcγRI R	CCA GCT CGA GAG GAG CTG ATG ACT GGG GAC CAA G
mFcγRII F	CCC AAG CTT ACT CAT GAT CTT CCA AAG GCT GTG GTC
mFcγRII R	CCA GCT CGA GTG GTA AAG ACC TGC TGG ACT TGG GC
mFcγRIII F	CCC AAG CTT GCT CTT CCG AAG GCT GTG GTG AAA C
mFcγRIII R	CCA GCT CGA GAG TGT GGT ACC AGA CTA GAG AGA TGG
mFcγRIV F	CCC AAG CTT GGT CTC CAA AAG GCT GTG GTG AAC C
mFcγRIV R	CCA GCT CGA GAT CGC CTA GGC TTA TAC GAA AGG ATG CT
E320D For	GAC TGG CTG AAT GGC AAG GAG TAC GAT TGC AAG GTC TCC AAC AAA GCC CTC
E320D Rev	GAG GGC TTT GTT GGA GAC CTT GCA ATC GTA CTC CTT GCC ATT CAG CCA GTC
R386K For	GTG GAG TGG GAG AGC AAT GGG AAG CCG GAG AAC AAC TAC AAG ACC ACA C
R386K Rev	GTG TGG TCT TGT AGT TGT TCT CCG GCT TCC CAT TGC TCT CCC ACT CCA C

Supplementary Table 2. EC_{50} values of OA801 and OA802 by CDC in Raji and Ramos cells. Data are average values ± SD.

	EC_{50} (nM)/Fold	Tumor cells
Ofatumumab	3.43 ± 1.90	Raji cells
OA801	1.83 ± 0.23 / 1.9	
OA802	2.30 ± 0.17 / 1.5	
Ofatumumab	0.25 ± 0.02	Ramos cells
OA801	0.06 ± 0.01 / 4.1	
OA802	0.11 ± 0.01 / 2.2	

Supplementary Table 3. Cγ2/Cγ3 dihedral-angles in IgG1 Fc domains in the PDB

	Cγ2/Cγ3 Dihedral-Angle (°)	
	Chain A	Chain B
A801	-20.5	136
G801	-21.1	-22.4
1FC1	-21	-24.6
1H3T	-33.1	-17.6
1H3U	-28.4	-27.7
1H3V	-30.5	-20.7
1H3W	-27.5	NA
1H3Y	-28.5	-20.4
1L6X	-22.8	NA
2DTS	-28.6	-28.9
3AVE	-29.2	-25.5
3DNK	-31.8	-24
3S7G	-18.4	-26.7